

Review of Lattice QCD calculations of kaon decays

Christopher Kelly^{a,*}

^a*Computational Science Institute, Brookhaven National Laboratory,
Upton, New York, USA.*

E-mail: ckelly@bnl.gov

We review the RBC & UKQCD collaborations' lattice calculation of direct CP-violation in neutral kaon decays. The results are compared to experiment and the Standard Model origin of the $\Delta I = 1/2$ rule is demonstrated. Our plans for future calculations are also presented.

*The 10th International Workshop on Chiral Dynamics - CD2021
15-19 November 2021
Online*

*Speaker

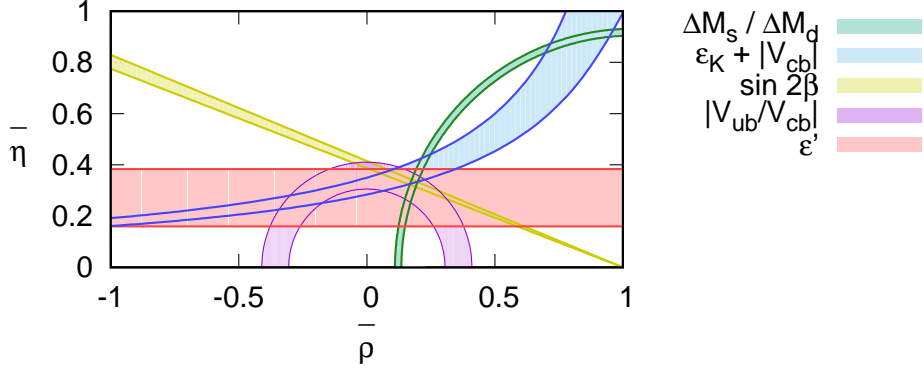


Figure 1: The CKM matrix unitarity triangle in the $\rho - \eta$ plane. The horizontal band is the constraint imposed by our calculation of ϵ' .

Lattice QCD is the only known systematically improvable (i.e. for which all systematic errors can be identified and reduced/eliminated with sufficient computational effort) technique for treating non-perturbative hadronic physics. In recent years lattice calculations have achieved a level of control and precision sufficient to directly aid experimental efforts in the search for new physics beyond the Standard Model (BSM). In the kaon sector particularly, lattice predictions for decay processes that are suppressed in the Standard Model – those for which BSM contributions can be relatively enhanced – have opened up a number of new avenues for searches on the Intensity Frontier including:

- Searches for new sources of flavor-changing neutral currents in the rare kaon decays $K \rightarrow \pi \nu \bar{\nu}$ and $K \rightarrow \pi l \bar{l}$. [1–3]
- Constraints on lepton flavor universality through leptonic kaon decays (“K12”). [4]
- Precision determination of the CKM matrix element $|V_{us}|$ through $K \rightarrow \pi$ semileptonic decays (“K13”). [5]
- Calculations of direct CP violation in $K \rightarrow \pi\pi$ decays.

A comprehensive review of many of these topics can be found in Ref. [6].

For this document we will focus upon the last item: the lattice calculation of direct CP-violation (CPV) in neutral kaon decays. These decays are highly suppressed in the Standard Model, and precise experimental results already exist, making this a highly attractive target for the search for new sources of CPV. These searches are motivated by the observation that explaining the predominance of matter over antimatter in the Universe via baryogenesis appears to require CPV in excess of Standard Model predictions. In addition, measurements of CPV in kaon decays also provide a new, horizontal band constraint on the CKM matrix unitarity triangle in the $\rho - \eta$ plane, as illustrated in Fig. 1 where we compare the constraint from our calculation versus those of other sources.

The first observations of direct CPV in kaon decays were performed in the late 1990s by the NA48 [8] and KTeV [9] experiments. The phenomenon is parameterized by ϵ' , the current world average of which is [10]

$$\text{Re}(\epsilon'/\epsilon) = 16.6(2.3) \times 10^{-4} \quad (1)$$

where ϵ is the measure of indirect CP-violation, itself heavily suppressed: $|\epsilon| = 2.228(11) \times 10^{-3}$. While the underlying weak interactions responsible for the decay occur at high energies, $O(80 \text{ GeV})$, the decay processes receive substantial corrections from low-energy hadronic physics that cannot be treated reliably with perturbation theory, hence it is only recently that precise Standard Model predictions have become feasible via lattice methods.

The RBC & UKQCD collaborations performed the first *ab initio* calculation of ϵ' in the Standard Model [11] in 2015 using lattice QCD with three quark flavors (u , d and s) and exact isospin symmetry ($m_u = m_d$). In this context ϵ' appears as the difference between the complex phases of the decay amplitudes of neutral kaons into two-pions in the isospin $I = 0$ (with amplitude A_0) and $I = 2$ (with amplitude A_2) representations,

$$\epsilon' = \frac{i\omega e^{i(\delta_2 - \delta_0)}}{\sqrt{2}} \left(\frac{\text{Im}A_2}{\text{Re}A_2} - \frac{\text{Im}A_0}{\text{Re}A_0} \right), \quad (2)$$

where $\omega = \text{Re}A_2/\text{Re}A_0$ and δ_I are the corresponding $\pi\pi$ scattering phase shifts. The following result was obtained,

$$\text{Re}(\epsilon'/\epsilon) = 1.38(5.15)(4.59) \times 10^{-4} \quad (3)$$

where the errors are statistical and systematic respectively. The observation of a tension at the 2.1σ level between the lattice and experimental results, and an unexplained tension of a similar size in the $I = 0$ $\pi\pi$ scattering phase shifts which form a necessary component of calculation, provided strong motivation for an improved calculation. A follow-up calculation of the $I = 0$ amplitude and ϵ' with a factor of two smaller statistical error, dramatically improved understanding and confidence in the systematic error resulting from the contribution of excited $\pi\pi$ states – resolving the phase-shift discrepancy – as well as several other important systematic error sources, was published in 2020 [7] and forms the basis of this document. We will also describe ongoing efforts to extend the calculation over the coming years.

1. Summary of the calculations

The low energy decay amplitudes are precisely described by first order weak effective theory,

$$A_I = \langle (\pi\pi)_I | H_W | K^0 \rangle, \quad (4)$$

where H_W is the three-flavor effective Hamiltonian,

$$H_W = \frac{G_F}{\sqrt{2}} V_{ud}^* V_{us} \sum_{i=0}^{10} [z_i(\mu) + \tau y_i(\mu)] Q_i(\mu), \quad (5)$$

which comprises ten effective four-quark operators Q_i , with Wilson coefficients z_i and y_i that encapsulate the high-energy contributions and are computed using perturbation theory. Here $\tau = -\frac{V_{ts}^* V_{td}}{V_{us}^* V_{ud}}$ contains the only imaginary contribution, which gives rise to the CP violation. While the Hamiltonian is renormalization scheme independent, the component four-quark operators and Wilson coefficients must be separately renormalized into a common scheme at a scale indicated by μ in the above. Conventionally the $\overline{\text{MS}}$ scheme is used for the computation of the Wilson coefficients. Unfortunately this scheme is not amenable to a lattice treatment as it involves fractional dimensions,

therefore an intermediate non-perturbative renormalization (NPR) scheme – one of the so-called RI-SMOM schemes – is utilized. A renormalization scale is chosen that is low enough to avoid discretization effects but high enough that the conversion factors relating the renormalized lattice amplitudes to the $\overline{\text{MS}}$ scheme can be computed reliably using perturbation theory. The existence of this window requires a compromise that can result in significant systematic errors arising from the truncation of the perturbative series in the matching calculation.

On the lattice the $K \rightarrow \pi\pi$ matrix elements are obtained by fitting to three-point functions of the form

$$C_i(t, t_{\text{sep}}^{K \rightarrow \text{snk}}) = \langle 0 | \mathcal{O}_{\text{snk}}^\dagger(t_{\text{sep}}^{K \rightarrow \text{snk}}) Q_i(t) \mathcal{O}_K(0) | 0 \rangle \quad (6)$$

where \mathcal{O}_K is the kaon operator, \mathcal{O}_{snk} creates the $\pi\pi$ state and Q_i are the four-quark operators discussed above. In the limit of large (Euclidean) times t and $t' = t_{\text{sep}} - t$ these correlation functions are described thus:

$$C_i(t, t_{\text{sep}}^{K \rightarrow \text{snk}}) \xrightarrow{t, t' \rightarrow \infty} \frac{1}{\sqrt{2}} A_K A_{\pi\pi} e^{-m_K t} e^{-E_{\pi\pi} t'} M_i \quad (7)$$

where $M_i = \langle \pi\pi | Q_i | K \rangle$, A_K and A_{snk} describe the overlap between the kaon and $\pi\pi$ states with their corresponding operators, m_K is the kaon mass, and $E_{\pi\pi}$ the $\pi\pi$ energy (which is equal to the kaon mass for a physical decay). Note that the renormalization and finite volume correction of M_i are required prior to their usage in Eqs. 4 and 5.

In practise the kaon and $\pi\pi$ operators project onto *all* states with the corresponding quantum numbers and care must be taken to isolate the states of interest. The contribution of each state falls exponentially in lattice time according to the energy of the state such that at large times the signal is dominated by only the lightest states. Nevertheless, excited state contamination remains a significant potential source of systematic error. A second challenge specific to this calculation is that with the typical periodic spatial boundary conditions (BCs), the spectrum of states generated by the $\pi\pi$ operator includes a state comprising two pions at rest. This has an energy ~ 260 MeV, lower than the kaon mass of ~ 500 MeV, hence an unphysical, energy nonconserving decay dominates the signal at large times. While multi-state fits to extract the subdominant physical contribution are possible, it is often very difficult to reliably isolate the excited-state terms, particularly with noisy data. For these calculations we instead exploit the ability to modify the lattice spatial BCs while incurring only exponentially-suppressed finite-volume errors: For the $I = 2$ calculation an isospin rotation relates the neutral kaon decay to $K^+ \rightarrow \pi^+ \pi^+$. The spatial BCs of the down-quark alone are then changed from periodic to antiperiodic, which results in the final state charged pions also becoming antiperiodic, hence their lattice momenta become discretized in odd-integer multiples of π/L where L is the lattice size. We can then tune L such that the lowest-energy state comprises two pions with a total energy that matches the kaon mass. This operation breaks the isospin symmetry, but any mixing of the final state is prevented by virtue of $\pi^+ \pi^+$ being the only allowed doubly-charged state. For the $I = 0$ calculation the isospin breaking in this approach cannot be avoided, therefore we employ instead G-parity BCs, for which a charge-conjugation and isospin rotation are performed at the lattice boundary. Both neutral and charged pions are negative under G-parity hence we achieve the same effect of imposing antiperiodic BCs but for all pions and without breaking isospin, at the cost of a significant increase in computational cost [12].

1.1 2015 calculations

The A_2 ($\Delta I = 3/2$) amplitude is composed of three linear combinations of the operators Q_i that are labeled by their representation under chiral $SU(3)_L \times SU(3)_R$. The dominant contributor to the real part is the $(27, 1)$ combination and the imaginary part is dominated by the remaining $(8, 8)$ combinations. The latest calculation [13] was performed in 2015 using physical quark masses, a large physical volume and hence good control over finite-volume errors, and two lattice spacings allowing a continuum limit to be taken. We obtained,

$$\text{Re}A_2 = 1.50(4)(14) \times 10^{-8} \text{ GeV} \quad (8a)$$

$$\text{Im}A_2 = -6.99(20)(84) \times 10^{-14} \text{ GeV} \quad (8b)$$

where the errors are statistical and systematic, respectively. A significant achievement of this calculation is obtaining a result with $< 1\%$ statistical errors despite having performed a continuum extrapolation. The systematic error is dominated entirely by perturbative truncation errors in the matching of our NPR scheme to $\overline{\text{MS}}$ (8%) and in the Wilson coefficients (12%). The result for $\text{Re}A_2$ is in good agreement with the experimental values of $\text{Re}A_2 = 1.4787(31) \times 10^{-8} \text{ GeV}$ from charged kaon decays and $1.570(53) \times 10^{-8} \text{ GeV}$ from neutral kaon decays.

The A_0 ($\Delta I = 1/2$) amplitude requires all ten effective four-quark operators; the operator Q_2 provides the dominant contribution to the real part and Q_6 , and to a lesser extent Q_4 , dominate the imaginary part. This is a considerably more computationally expensive calculation than A_2 , not just due to the added cost of G-parity boundary conditions but also because the vacuum quantum numbers of the final state result in the presence of disconnected diagrams that are inherently noisy, requiring larger statistics and more sophisticated methods to adequately resolve. As a result, for the first calculation of A_0 , also performed in 2015 [11], we used only a single lattice with a relatively coarse lattice spacing, allowing us to have good control over finite-volume errors at the cost of larger discretization errors. A single $\pi\pi$ operator, labeled $\pi\pi(111)$, was chosen in which the two pions are generated moving back-to-back with momentum $(\pm 1, \pm 1, \pm 1)\pi/L$. We obtained

$$\text{Re}A_0 = 4.66(1.00)(1.26) \times 10^{-7} \text{ GeV} \quad (9a)$$

$$\text{Im}A_0 = -1.90(1.23)(1.08) \times 10^{-11} \text{ GeV} . \quad (9b)$$

The larger relative statistical error on the imaginary part arises primarily from a strong cancelation between the dominant Q_4 and Q_6 contributions. While this calculation had substantial, $\mathcal{O}(12\%)$ discretization errors due to the coarse lattice spacing, the systematic error is again dominated by perturbative truncation errors. The real part is in agreement with the experimental value $\text{Re}A_0 = 3.3201(18) \times 10^{-7} \text{ GeV}$.

Combining the above results for A_0 and A_2 using Eq. (2), we found

$$\text{Re}(\epsilon'/\epsilon) = 1.38(5.15)(4.59) \times 10^{-4}, \quad (10)$$

which is 2.1σ below the experimental value. While the errors on the calculation are large, roughly $3\times$ those of the experiment, this result clearly demonstrates that ϵ' is now accessible to lattice calculation.

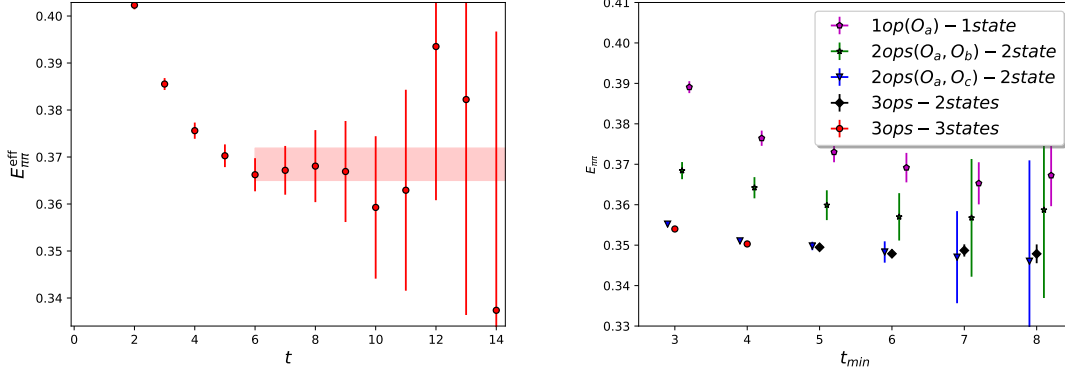


Figure 2: (Left) The $\pi\pi$ effective energy obtained using 1438 configurations with the $\pi\pi(111)$ operator. (Right) The fitted $I = 0$ $\pi\pi$ energy obtained using multiple operators and 741 configurations, varying the lower bound on the fit range t_{\min} , the number of operators and number of states. In the legend O_a , O_b , O_c correspond to the $\pi\pi(111)$, $\pi\pi(311)$ and σ operators, respectively. Our best fit is the 3-operator, 2-state result with $t_{\min} = 6$.

1.2 Updated calculation of A_0 [7]

As previously mentioned, the tension between the calculation of ϵ' and experiment was accompanied by a similar tension in the $I = 0$ $\pi\pi$ scattering phase shift; we obtained $\delta_0(E_{\pi\pi} \approx m_K) = 23.8(4.9)(1.2)^\circ$, roughly 3σ smaller than the prediction of $\sim 39^\circ$ obtained by combining the dispersive Roy equations with experimental input [14]. Both the phase-shift and the associated $\pi\pi$ energy are key ingredients of the calculation, therefore it is crucial that a reliable result is obtained. Following the 2015 publication we sought to address this issue by increasing the statistics by almost $7\times$, but found that the disagreement (in units of the error) became worse in doing so, producing a value of $19.1(2.5)^\circ$ [15]. The corresponding effective mass plot, the plateau value of which indicates the ground-state energy, is reproduced in Fig. 2. We observe what appears to be a clear plateau, but nevertheless the most likely explanation for the discrepancy is excited state contamination arising from a second state with an energy close to that of the ground-state, whose contribution is masked by the rapid growth of the error bars.

To address the potential excited-state contamination we performed measurements on 741 configurations ($3.4\times$ the number used for the original calculation) with two additional $\pi\pi$ operators: the $\pi\pi(311)$ operator in which the two pions again move back-to-back but with momenta $(\pm 3, \pm 1, \pm 1)\pi/L$ and permutations thereof, and the scalar $\sigma = (\bar{u}u + \bar{d}d)/\sqrt{2}$ operator. By varying the source and sink operators we can construct a matrix of correlation functions whose time dependence can be fit simultaneously to extract the energies and amplitudes of multiple $\pi\pi$ states with considerably higher precision and control than relying on the large-time dependence of a single operator. This is evidenced by Fig. 2 where we show the fitted $\pi\pi$ energy as we vary the fit range, the number of operators and the number of fitted states; a clear advantage is observed both in the statistical error and the quality of the plateau as additional operators are included. We obtained [15]

$$\delta_0(471 \text{ MeV}) = 32.3(1.0)(1.4)^\circ, \quad (11)$$

which is in much better agreement with the dispersive prediction at this energy of 35.9° . We

therefore conclude that excited state contamination was indeed responsible for the disagreement and that it has now been resolved.

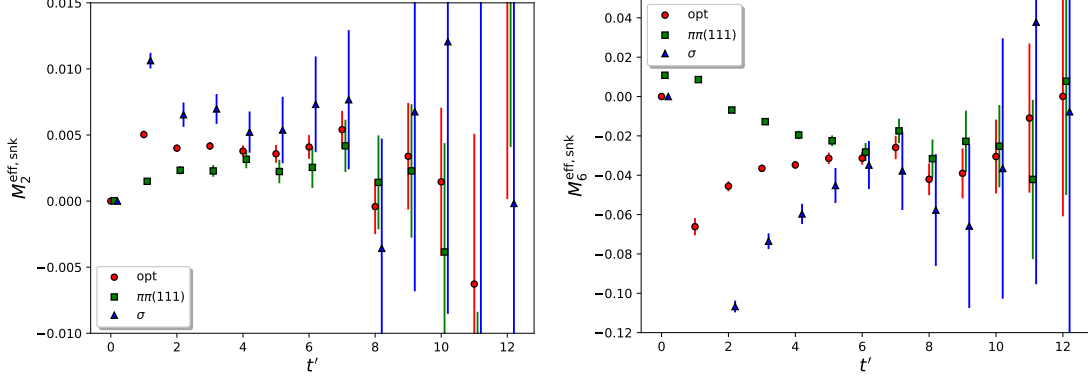


Figure 3: The effective matrix elements of the Q_2 and Q_6 operators for the $\pi\pi(111)$, σ and optimal operators as a function of the time separation t' between the four-quark operator and the $\pi\pi$ sink operator.

We also observed a considerable improvement in the $K \rightarrow \pi\pi$ matrix elements: In Fig 3 we plot the effective matrix elements defined as,

$$M_i^{\text{eff,snk}}(t') = C_i(t, t_{\text{sep}}^{K \rightarrow \text{snk}}) \left(\frac{1}{\sqrt{2}} A_K A_{\text{snk}}^0 e^{-m_K t} e^{-E_0 t'} \right)^{-1} = M_i^0 + \sum_j \frac{A_{\text{snk}}^j}{A_{\text{snk}}^0} M_i^j e^{-(E_j - E_0) t'}. \quad (12)$$

where $t' = t_{\text{sep}}^{K \rightarrow \text{snk}} - t$ and C_i are defined in Eq. 6. Here A_K and m_K are again the ground-state kaon amplitude and mass, and A_{snk}^j and E_j are amplitudes and energies of the states created by the $\pi\pi$ operator. Both the amplitudes and energies are obtained from their respective two-point function fits. A uniform cut of $t_{\text{min}} = 6$ is applied to isolate the kaon ground state contribution. As indicated, $M_i^{\text{eff,snk}}$ converge to the desired matrix elements M_i^0 at large t' . In the figure we compare the $\pi\pi(111)$ and σ effective matrix elements against the optimal combination of those two operators that best projects onto the ground state. As with $\pi\pi$ fits, we observe that the additional operators dramatically improve the statistical error and the length and quality of the plateau.

In Fig. 4 we plot the fit results for the Q_2 and Q_6 operators, which dominate the real and imaginary parts of A_0 , respectively, as we vary the number of operators, states and the temporal cuts. For Q_2 we find good agreement between all of the fits for $t'_{\text{min}} \geq 4$, although improved statistical errors are obtained with the additional operators. However for Q_6 we see a clear pattern of excited state contamination in the one and two-operator fit results, the latter converging earlier than the former as we would expect. For our final best fit we took the result with three operators and two states with $t'_{\text{min}} = 5$ and $t_{\text{min}} = 6$. The measurement strategy used for the 2015 calculation corresponds to the “ 1×1 $t_{\text{min}} = 6$ ” point with $t'_{\text{min}} = 4$ which is incompatible with our new result, implying that the $\leq 5\%$ excited state systematic error was significantly underestimated.

The updated calculation includes a further refinement in the use of “step-scaling” [16] for the non-perturbative renormalization, which allows the limit on the largest renormalization scale imposed by the lattice spacing to be circumvented by incorporating the non-perturbative running computed on a finer lattice between a low scale accessible on the coarse lattice and a higher scale.

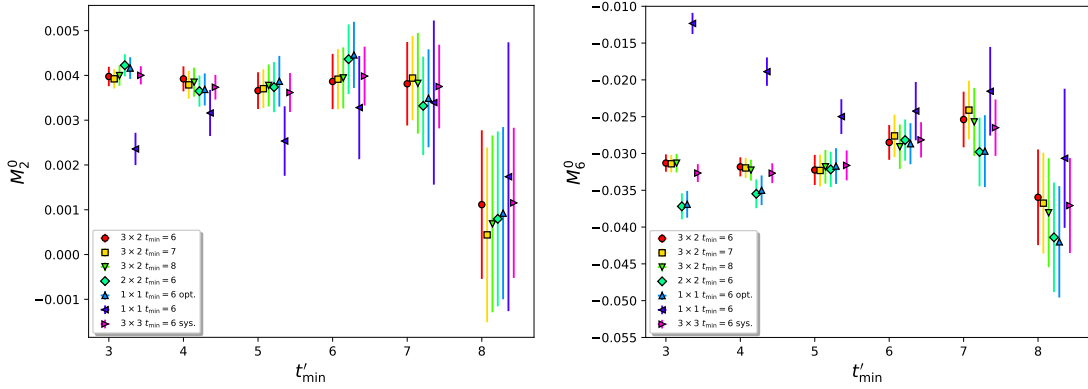


Figure 4: The fitted ground-state matrix elements of the Q_2 and Q_6 operators for various choices of the number of operators, number of states and the cut t_{\min} between the kaon and four-quark operators, as a function of the cut t'_{\min} between the four-quark operator and the $\pi\pi$ sink. In the legend “ $a \times b$ ” indicates the fit was performed with a operators and b states, and “opt.” indicates the optimal operator was used. In the two-operator case we drop the $\pi\pi(311)$ operator and in the one-operator case we further drop the σ . The “sys.” results are obtained using three operators and three states for both the $\pi\pi$ and $K \rightarrow \pi\pi$ fits and is used in the systematic error estimation. The values are shifted for clarity.

Using this technique we increased our renormalization scale from 1.53 GeV to 4 GeV, reducing the estimated 15% truncation systematic error in the $\overline{\text{RI}} \rightarrow \overline{\text{MS}}$ matching by a factor of $3\times$. Unfortunately a corresponding decrease in the systematic error arising from the use of perturbation theory for the Wilson coefficients was not obtained despite their also being evaluated at this high scale, primarily due to the underlying use of perturbation theory to match between the 4- and 3-flavor theories at the charm mass scale $m_c \approx 1.3$ GeV.

2. Results of the updated calculation

2.1 The $\Delta I = 1/2$ rule

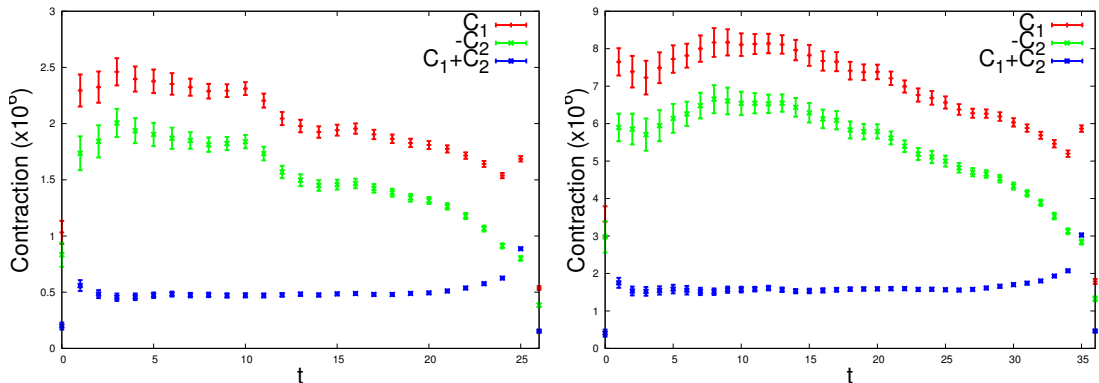


Figure 5: The two dominant contributions C_1 and C_2 to $\text{Re}A_2$ and their sum on the 48I (left) and 64I (right) ensembles, reproduced from Fig. 11 of Ref. [13].

Experimental results show that the $\Delta I = 1/2$ decay is roughly ~ 500 more common than the $\Delta I = 3/2$ decay, which is reflected in the ratio

$$\frac{1}{\omega} = \frac{\text{Re}A_0}{\text{Re}A_2} = 22.45(6), \quad (13)$$

the inverse of which appears as a coefficient in the equation for ϵ' , Eq. (2). The origin of this $\Delta I = 1/2$ rule has been a longstanding mystery. A factor of two difference can be accounted for by the perturbative running from the weak to the charm scales, but there has been no widely accepted explanation as to the origin of the remaining factor of ten. Our lattice calculation provides an answer: the two largest diagrams C_1 and C_2 contributing to the $(27, 1)$ operator which dominates $\text{Re}A_2$ strongly cancel, as illustrated in Fig. 5. This behavior is counter to that predicted by naïve color counting which suggests these terms should have the same sign and differ by a factor of three in size. Combining our A_0 and A_2 calculations we find

$$\frac{1}{\omega} = \frac{\text{Re}A_0}{\text{Re}A_2} = 19.9(5.0) \quad (14)$$

which is completely consistent with the experimental number, hence we conclude that the $\Delta I = 1/2$ rule is a consequence of low-energy QCD.

2.2 A_0 and ϵ'

For the $\Delta I = 1/2$ amplitude we obtain

$$\text{Re}A_0 = 2.99(0.32)(0.59) \times 10^{-7} \text{ GeV} \quad (15a)$$

$$\text{Im}A_0 = -6.98(0.62)(1.44) \times 10^{-11} \text{ GeV} \quad (15b)$$

The real part agrees well with the experimental result $\text{Re}A_0 = 3.3201(18) \times 10^{-7} \text{ GeV}$ and with our previous result, however the value for the imaginary part differs substantially from our 2015 calculation, giving rise to a similarly large change in ϵ' :

$$\text{Re}(\epsilon'/\epsilon) = 21.7(2.6)(6.2)(5.0) \times 10^{-4}, \quad (16)$$

where the first set of parentheses gives the statistical error. Here the systematic error has been separated into two, with the third set of parentheses corresponding to an estimate (23%) of the effects of isospin breaking (IB) and electromagnetism (EM) obtained through next-to-leading order chiral perturbation theory with input from the $1/N_c$ expansion [17]. EM+IB effects typically enter at the percent scale in hadronic quantities, but for $K \rightarrow \pi\pi$ their relative effects are enhanced due to the $20\times$ suppression of A_2 by the mechanics of the $\Delta I = 1/2$ rule. We did not previously include these effects in our error budget as the result was considered a pure-QCD calculation. The remaining systematic error is given by the second set of parentheses and is dominated by the discretization error (12%) and the perturbative truncation error in the Wilson coefficients (12%). The excited state systematic error is treated as negligible compared to the other sources of error given the control over such effects provided by the multi-operator method demonstrated in the previous section.

This result for $\text{Re}(\epsilon'/\epsilon)$ is now in good agreement with the experimental number.

3. Conclusions and outlook

Recent advances in techniques and computational power have brought about a golden age where lattice calculations of kaonic quantities can have a significant impact on the search for new physics. This document detailed the RBC & UKQCD collaboration's calculation of CP-violation $K \rightarrow \pi\pi$ decays, primarily focusing on a recent, updated calculation [7] of the $\Delta I = 1/2$ amplitude A_0 following from our original 2015 calculation [11]. Among the notable changes are a $3.4\times$ increase in statistics; the addition of two more $\pi\pi$ operators to the data which vastly improves our control over excited state effects, resolving a discrepancy previously observed between the lattice and dispersive predictions of the $I = 0$ $\pi\pi$ scattering phase shift at the kaon mass scale as well as improving the statistical error and the quality of the plateaus; and the use of step-scaling to raise the renormalization scale from 1.53 GeV to 4 GeV resulting in a $3\times$ improvement in the formerly-dominant error resulting from the $\overline{\text{MS}}$ matching. By combining the results with our earlier calculation of A_2 we obtain an *ab initio* determination of $\text{Re}A_0/\text{Re}A_2$ that is consistent with experiment and thus demonstrate that the $\Delta I = 1/2$ rule mainly arises from non-perturbative QCD effects. We also obtain a result for $\text{Re}(\epsilon'/\epsilon)$ that is now consistent with the experimental value and has a total error that is $\sim 3.6\times$ that of the experiment.

We believe that ϵ' remains a promising avenue in which to search for new physics, but improvements in the systematic errors are required. The single largest source of error is from the missing contributions of isospin breaking and electromagnetism. Unfortunately the lattice treatment of electromagnetism is complicated by the long-range nature of the interactions and so theoretical hurdles must be overcome before a first principles calculation is possible. We are presently exploring a novel technique for treating the interactions using a truncated potential in Coulomb gauge where the truncation range is set to confine the interaction within the finite box resulting in finite-volume errors that can be treated analytically using infinite-volume perturbation theory [18].

A second significant source of error arises from the use of perturbation theory to match between the four- and three-flavor effective theories in the Wilson coefficients. While a four-flavor lattice calculation with physical charm quarks is possible, the requirement of large statistics, a fine lattice spacing to control charm discretization effects and a large volume to control finite-volume effects puts this outside of the reach of present and near-future supercomputers. In the interim we are investigating the possibility of computing the $4 \rightarrow 3f$ matching non-perturbatively [19, 20].

The dramatic improvement in control over excited state effects that we discussed in this document has reopened the question as to whether we can perform multi-state fits to extract the physical $\Delta I = 1/2$ matrix element from a calculation with periodic boundary conditions, forgoing the use of the computationally-expensive G-parity boundary conditions to remove the dominant contribution of the unphysical decay of the kaon to a stationary $\pi\pi$ state. We are presently conducting a preliminary calculation on two different coarse lattices to evaluate this approach [21].

Finally, the largest pure-lattice systematic error is due to the fact that A_0 has only been computed at a single, somewhat coarse lattice spacing. We are presently generating two additional ensembles with G-parity boundary conditions which will allow for the controlled continuum extrapolation of our result for A_0 [22], largely eliminating this source of error.

References

- [1] N. H. Christ *et al.* [RBC and UKQCD], Phys. Rev. D **100**, no.11, 114506 (2019) doi:10.1103/PhysRevD.100.114506 [arXiv:1910.10644 [hep-lat]].
- [2] N. H. Christ, X. Feng, L. C. Jin and C. T. Sachrajda, Phys. Rev. D **103**, no.1, 014507 (2021) doi:10.1103/PhysRevD.103.014507 [arXiv:2009.08287 [hep-lat]].
- [3] N. H. Christ, X. Feng, L. Jin, C. Tu and Y. Zhao, PoS **LATTICE2019**, 128 (2020) doi:10.22323/1.363.0128
- [4] A. Bazavov *et al.* [Fermilab Lattice and MILC], Phys. Rev. D **99**, no.11, 114509 (2019) doi:10.1103/PhysRevD.99.114509 [arXiv:1809.02827 [hep-lat]].
- [5] A. Bazavov, C. Bernard, N. Brown, C. Detar, A. X. El-Khadra, E. Gámiz, S. Gottlieb, U. M. Heller, J. Komijani and A. S. Kronfeld, *et al.* Phys. Rev. D **98**, no.7, 074512 (2018) doi:10.1103/PhysRevD.98.074512 [arXiv:1712.09262 [hep-lat]].
- [6] Y. Aoki, T. Blum, G. Colangelo, S. Collins, M. Della Morte, P. Dimopoulos, S. Dürr, X. Feng, H. Fukaya and M. Golterman, *et al.* [arXiv:2111.09849 [hep-lat]].
- [7] R. Abbott *et al.* [RBC and UKQCD], Phys. Rev. D **102**, no.5, 054509 (2020) doi:10.1103/PhysRevD.102.054509 [arXiv:2004.09440 [hep-lat]].
- [8] J. R. Batley *et al.* [NA48], Phys. Lett. B **544**, 97-112 (2002) doi:10.1016/S0370-2693(02)02476-0 [arXiv:hep-ex/0208009 [hep-ex]].
- [9] E. Abouzaid *et al.* [KTeV], Phys. Rev. D **83**, 092001 (2011) doi:10.1103/PhysRevD.83.092001 [arXiv:1011.0127 [hep-ex]].
- [10] M. Tanabashi *et al.* [Particle Data Group], Phys. Rev. D **98**, no.3, 030001 (2018) doi:10.1103/PhysRevD.98.030001
- [11] Z. Bai *et al.* [RBC and UKQCD], Phys. Rev. Lett. **115**, no.21, 212001 (2015) doi:10.1103/PhysRevLett.115.212001 [arXiv:1505.07863 [hep-lat]].
- [12] N. H. Christ, C. Kelly and D. Zhang, Phys. Rev. D **101**, no.1, 014506 (2020) doi:10.1103/PhysRevD.101.014506 [arXiv:1908.08640 [hep-lat]].
- [13] T. Blum, P. A. Boyle, N. H. Christ, J. Frison, N. Garron, T. Janowski, C. Jung, C. Kelly, C. Lehner and A. Lytle, *et al.* Phys. Rev. D **91**, no.7, 074502 (2015) doi:10.1103/PhysRevD.91.074502 [arXiv:1502.00263 [hep-lat]].
- [14] G. Colangelo, J. Gasser and H. Leutwyler, Nucl. Phys. B **603**, 125-179 (2001) doi:10.1016/S0550-3213(01)00147-X [arXiv:hep-ph/0103088 [hep-ph]].
- [15] T. Blum *et al.* [RBC and UKQCD], [arXiv:2103.15131 [hep-lat]].
- [16] R. Arthur *et al.* [RBC and UKQCD], Phys. Rev. D **83**, 114511 (2011) doi:10.1103/PhysRevD.83.114511 [arXiv:1006.0422 [hep-lat]].

- [17] V. Cirigliano, H. Gisbert, A. Pich and A. Rodríguez-Sánchez, *JHEP* **02**, 032 (2020) doi:10.1007/JHEP02(2020)032 [arXiv:1911.01359 [hep-ph]].
- [18] J. Karpie, PoS **LATTICE2021**, 312 (2021)
- [19] M. Tomii, PoS **LATTICE2018**, 216 (2019) doi:10.22323/1.334.0216 [arXiv:1901.04107 [hep-lat]].
- [20] M. Tomii, PoS **LATTICE2019**, 174 (2020) doi:10.22323/1.363.0174
- [21] M. Tomii, PoS **LATTICE2021**, 394 (2021)
- [22] C. Kelly, PoS **LATTICE2021**, 008 (2021)